PEOPLE'S DEMOCRATIC REPUBLIC OF ALGERIA
MINISTRY OF HIGHER EDUCATION AND SCIENTIFIC RESEARCH

Mohamed El-Bachir El-Ibrahimi University - Bordj Bou Arreridj
Faculty of Science and Technology

department of Electronic

Thesis

Presented to obtain
THE MASTER'S DEGREE
Field: **Electronic**
Specialty: Micro-Electronic
by

➢ **Fahmi Mokhtara**

Entitled

study of the optoelectronic properties of an $Al_xGa_{1-x}As$ ternary semiconductor alloy.

Defended on : 02/07/2023

Before Jury committee:

Last and First Name	*Grade*	*Quality*	*Affiliation*
Dr Kherrat Fadila	*MAA*	*President*	*Univ-BBA*
Dr Fares Fahima	*MCA*	*Supervisor*	*Univ-BBA*
Dr A.Djemouai	*MCB*	*Examiner*	*Univ-BBA*

academic year 2022/2023

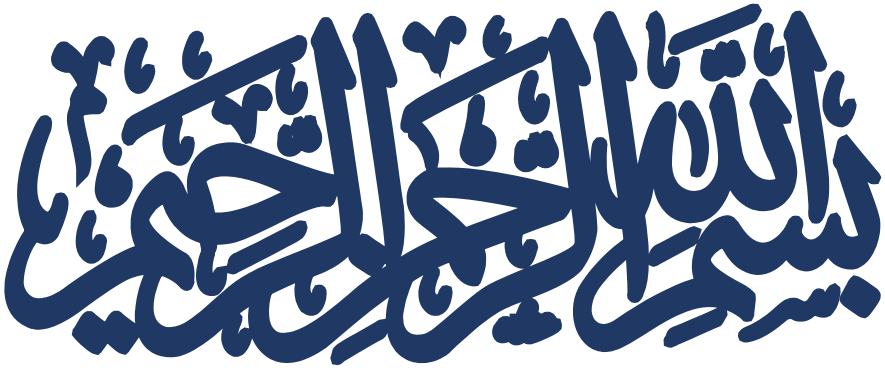
بسم الله الرحمن الرحيم

ACKNOWLEDGMENTS

«Praise to Allah, who has guided us to this; and we would never have been guided if Allah had not guided us»

First, I would like to thank Allah for giving me the strength, audacity and endurance to realize this work.

Second, I would like to express my thanks and gratitude to Dr Fahima Fares, my supervisor, who supported me throughout achievement of this work. I also thank her for all the scientific and technical information and her educational experience sharing, during my study in this Master degree.

My special thanks to the jury members who devoted their precious time and efforts to reading and correcting my work.

Also, I want to thank my colleagues for their help in gathering the necessary information needed for the practical part in this Dissertation.

I also don't forget my cousin Dr. M. Charafeddine, who was my brother's mentor and supporter of me and who was always by my side encouraging me to give more. I also thank my friend Yagoub TakiyEddin, who helped me get this work done. Thnak you so much my friend “Z.Abdelouakil”, ”S.N” and “B.I” , and “C.B”.

To all my friends and my family thank you for sharing with me the good and bad moments; thank you for your encouragement and support.

Dedication

I dedicate this work to

My parents,
sisters, and
brothers.

To all those who love me.

Table of Contents

Chapter II Methods for calculating energy bands

Chapter 03: results and discussions

General conclusion

List of Figures

List of Tables

General Introduction

General introduction

Semiconductor technology revolutionized various industries, including telecommunications, energy, automobiles, and health care. It continues to progress rapidly, with the development of new materials and manufacturing techniques to improve the performance and efficiency of electronic devices. In short, semiconductors are materials that possess intermediate electrical properties between conductors and insulators. Its unique properties allow controlled manipulation of electric current, making it indispensable for modern electronics and technology.

From recent semiconductor discoveries that have thrived in the technical and technological field, one of the most famous is silicon material, which is the most popular material used in the electronic market due to space reduction and weight reduction.

One of the reasons semiconductors have become the material of choice for the electronics industry is the existence of very sophisticated growth techniques. Their industrial applications, in turn, have led to the increasing sophistication of these techniques **[1]**.

Today, compound III-V semiconductors form the material basis for several well-established commercial technologies, as well as new types of advanced electronic and optoelectronic devices. Just a few examples include high electron mobility and heterostructure bipolar transistors, laser diodes, light-emitting diodes, photodetectors, photoelectric modulators, and mixing components. Frequency **[2]**.

AlGaAs material provides many advantages compared to the all-silicon technology, among which are the electrical and structural properties that give us the best performance and the lowest energy, but these compounds have been (still) under study and work.

This thesis aims to review one of these new compounds that are still under study and development, in which, we focused our study on ternary compounds, such as AlGaAs. Through this work, we will try to answer a research question about the compound's electrical and optical properties and its important quantitative features. Here, we have used the empirical method of pseudo potential (EPM), and virtual crystal approximation (VCA) .

The remainder of the thesis is structured as follows:

- In the first chapter we focused on introducing the theoretical concepts and generalities of semiconductors and their properties.
- In the second chapter, we have highlighted methods for calculating energy bands.
- In the last chapter we have done the practical side of the work.
- Finally, we put a general conclusion to the work

Chapter I

General notions about semiconductors

I.1. Introduction

Semiconductors are a special type of material that can conduct electricity under certain conditions. They are different from conductors, like metals, which allow electricity to flow easily, and insulators, like plastics or ceramics, which don't conduct electricity well.

Semiconductors are usually made of elements from the periodic table, such as silicon or germanium. These materials have a unique atomic structure that gives them their special electrical properties. Atoms in a semiconductor are arranged in a crystal structure, which means they form a repeating pattern.

Ternary semiconductor alloys refer to materials composed of three different elements, typically from the periodic table, in a solid-state crystal structure. These alloys offer unique properties and are widely used in various electronic and optoelectronic applications.

The composition of a ternary semiconductor alloy is typically denoted using the chemical symbols of the constituent elements. For example, AlGaAs represents an alloy composed of aluminum (Al), gallium (Ga), and arsenic (As). The proportions or ratios of these elements can be varied to tune the properties of the alloy.

Ternary semiconductor alloys find extensive applications in electronic devices, optoelectronics, and photovoltaics. For instance, alloys like InGaAsP and AlInGaP are used in light-emitting diodes (LEDs) and laser diodes for various wavelengths in the visible and infrared spectrum. These alloys enable the fabrication of efficient and tunable light sources.

I.2. Semiconductors in general

A semiconductor is a crystalline object whose conductive properties are intermediate between insulators and conductors, which vary greatly under the nuances of external environmental factors (temperature, pressure, etc.), presence of impurities (doping, lattice defects), and light **[3]**.

Semiconductors are a group of materials having conductivities between those of materials and insulators. Two general classify cations of semiconductors are the elemental semiconductor materials, found in group IV of the periodic table, and the compound semiconductor materials, most of which are formed from special combinations of group III and group V elements. **Table I.1** shows a portion of the periodic table in which the more common semiconductors are found

and **Table I.2** lists a few of the semiconductor materials. (Semiconductors can also be formed from combinations of group II and group VI elements, but in general these will not be considered in this text.)

The elemental materials, those that are composed of single species of atoms, are silicon and germanium. Silicon is by far the most common semiconductor used in integrated circuits and will be emphasized to a great extent.

The two-element, or binary, compounds such as gallium arsenide or gallium phosphide are formed by combining one group III and one group V element. Gallium arsenide is one of the more common of the compound semiconductors. Its good optical properties make it useful in optical devices. GaAs is also used in specialized applications in which, for example, high speed is required.

We can also form a three-element, or ternary, compound semiconductor. An example is Alx Ga1-x As, in which the subscript x indicates the fraction of the lower atomic number element component. More complex semiconductors can also be formed that provide flexibility when choosing material properties **[4]** .

Table I.1:A portion of the periodic table **[4]**

III	IV	V
5 **B** Boron	6 **C** Carbon	
13 **Al** Aluminum	14 **Si** Silicon	15 **P** Phosphorus
31 **Ga** Gallium	32 **Ge** Germanium	33 **As** Arsenic
49 **In** Indium		51 **Sb** Antimony

Table I.2: A list of some semiconductor materials **[4]**

Elemental semiconductors	
Si	Silicon
Ge	Germanium
Compound semiconductors	
AlP	Aluminum phosphide
AlAs	Aluminum arsenide
GaP	Gallium phosphide
GaAs	Gallium arsenide
InP	Indium phosphide

I.2.1 The notion of energy bands

The electrical behavior of semiconductors is often modeled using band theory which is a quantum model in solid state physics that determines the allowable energies of electrons in a solid and helps to understand the concept of electrical conductivity. This theory comes from the theory of molecular orbitals.

I.2.2 Band gap (energy gap)

In semiconductors as well as in insulators, the energy difference between the conduction and valence bands is called the band gap, or simply the gap noted as Eg, in which no particles can be found. carry electricity.

It is a fundamental parameter that determines the electronic and optical properties of semiconductors and thus evaluates their field of application.

The band structure of the semiconductor is compared with that of the insulator and metal, using the energy diagram in Figure I.1 **[3]**.

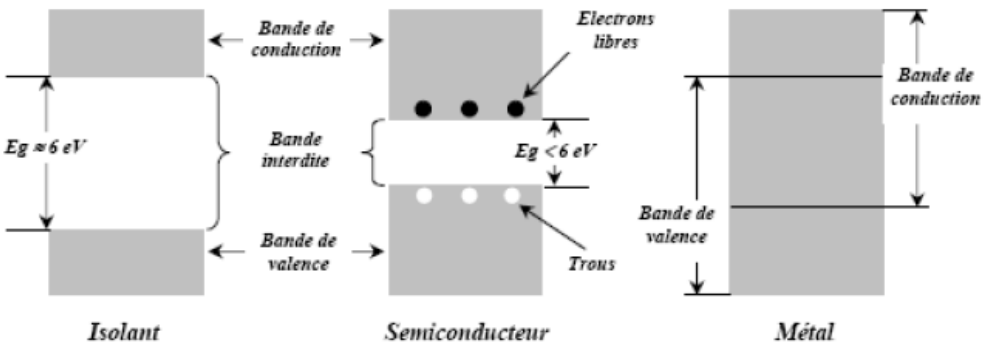

Figure I.1 Energy band structure of materials; insulators, semiconductors and metals **[3]**

I.2.3 Different types of semiconductors

There are two different types of semiconductors possible. One is called N-type material, and the other, P-type material. Unsurprisingly, the N stands for Negative and the P stands for Positive. N-type material is created by adding pentavalent impurities, that is, a dopant with five electrons in its outer shell.

c- N-type semiconductors

Figure **1.2** shows a silicon crystal pattern with a pentavalent impurity in its center. Compared to a common silicon atom with four electrons in its outer shell, a pentavalent impurity produces an extra electron, or donor. Therefore, the crystal has a negative charge and is called an N-type material. The energy level of the donor electrons lies just below the bottom of the conduction band. In other words, the difference between the donor and bottom of the conduction band is much smaller than the band gap itself.

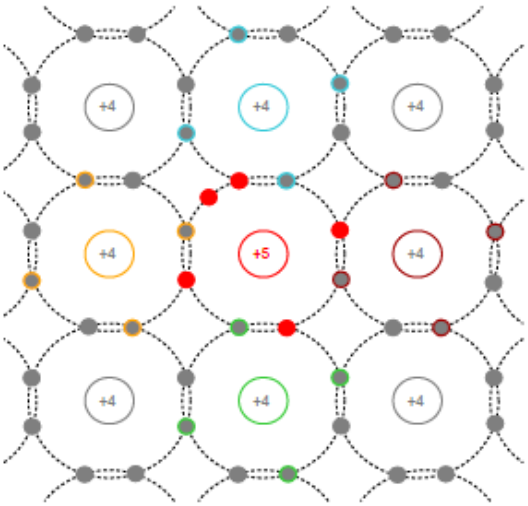

Figure 1.2 Crystal with added pentavalent impurity (N-type) **[5]**

This is illustrated in Figure 1.3 Notice how close the donor level is to the conduction band and how the Fermi level has been pushed up, away from the valence band and closer to the conduction band. This will be of great importance in future semiconductor device discussions.

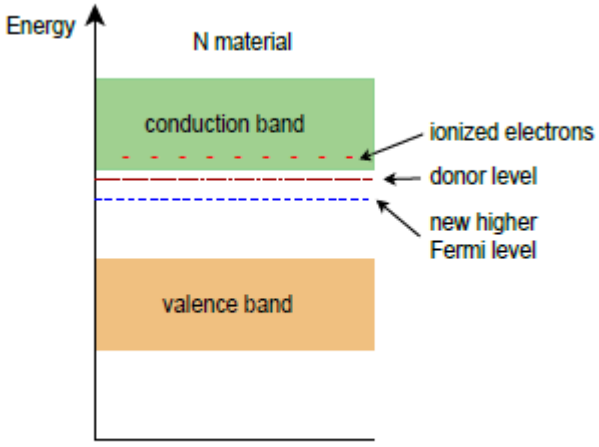

Figure 1.3 Energy band diagram of N-type semiconductor **[5]**

d- P-type semiconductors

Similarly, if we introduce a trivalent impurity, our crystal model now has a hole; electron shortage. For this reason, trivalent impurities are sometimes referred to as acceptors. The obtained crystal model is shown in Figure 1.4.

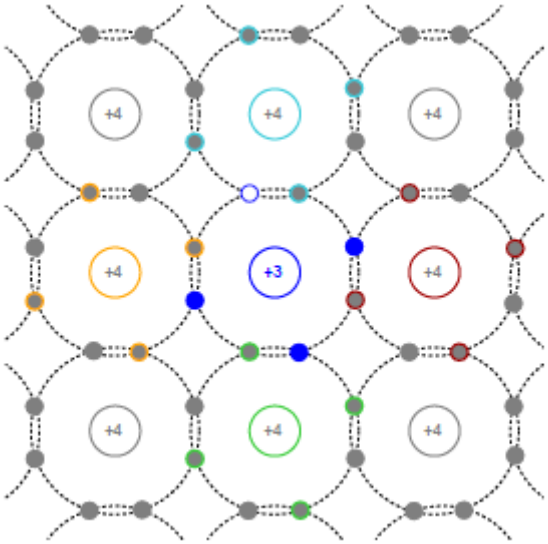

Figure 1.4 Crystal with added trivalent impurity (P-type) **[5]**

The resulting situation is essentially the opposite for n-type materials. Figure 1.5 shows the energy band diagram for the new p-type material. In this case, the Fermi level has been pushed low, closer to the valence band **[5]**.

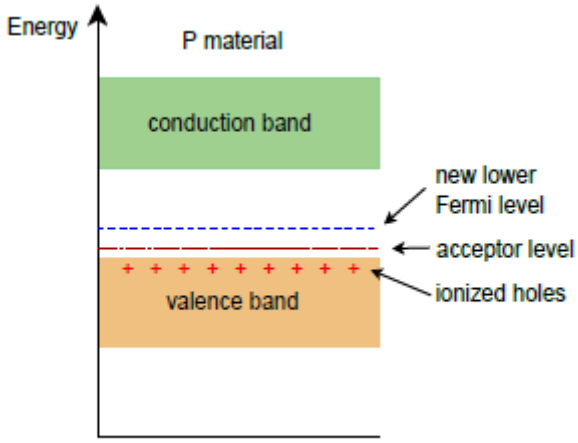

Figure 1.5 Energy band diagram of P-type semiconductor **[5]**

I.2.4 III-V semiconductors

III-V semiconductor materials are composite bodies formed from an element of the III (th) column and an element of the V (th) column of the periodic classification mendeleyev. Table II-1 contains an excerpt from this classification (the figures at the top and bottom represent the atomic number and the atomic mass respectively). Thus many binary compounds can be made

A semiconductor can be obtained if the sum of the electrons of the two species is equal to 8 electrons.

Table I.3: Extract from the periodic classification of elements **[6]**

III	IV	V
$^{5}_{10,81}B$	$^{6}_{12,01}C$	$^{7}_{14,01}N$
$^{13}_{26,98}Al$	$^{14}_{28,09}Si$	$^{15}_{30,97}P$
$^{31}_{69,74}Ga$	$^{32}_{72,59}Ge$	$^{33}_{74,92}As$
$^{49}_{114,82}In$	$^{50}_{118,69}Sn$	$^{51}_{121,75}Sb$

Table I.3 shows a simplified representation of the Mendeleyev periodic table to identify possible compounds and alloys.

For example:

Ga: the valence electron number is 3 electrons.

As: the valence electron number is 5 electrons.

Therefore:

Ga + As = GaAs: is a semiconductor because the sum of the electrons of the two species (Ga and As) is equal to 08 electrons. As (GaAs) it meets the condition of Bragg ($2d \sin q = nl$). Which represents the electron displacement law **[6]** .

I.3. Properties of semiconductor

I.3.1 Structural Properties

I.3.1.1 Structure cristalline Zinc Blende

Most binary III-V semiconductor materials and some II-VI materials have a Zinc-Blende (ZB) structure. In fact, in this phase, the primitive cell has two atoms, a cation of an element III and an anion of an element V by occupying the positions (0,0,0) and (1/4,1/4,1/4) respectively This structure consists of two face-centered cubic (fcc) sublattices (Figure I.6).The first Brillouin zone for the zinc-blende structure has the shape of a truncated octahedron (Figure I.7) **[7]**.

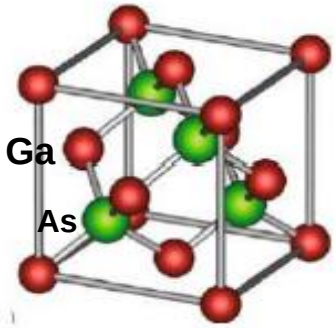

Figure I.6 Zinc-Blende structure (ZB) **[7]**

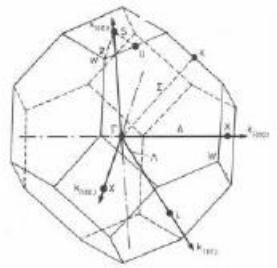

Figure I.7 First area of Brillouin **[7]**

Zincblende is characterized as a cubic closet packing (ccp), also known as face-centered cubic, structure.This crystal lattice structure is shown in **Figures I.8 & I.9** below. The discussion of corresponding zincblende and wurtzite states is helpful in understanding the nature of the energy

states in mixed crystals: (wurtzite structure [111] twinned on zincblende), and in faulted crystals: [111] stacking faults **[8]**.

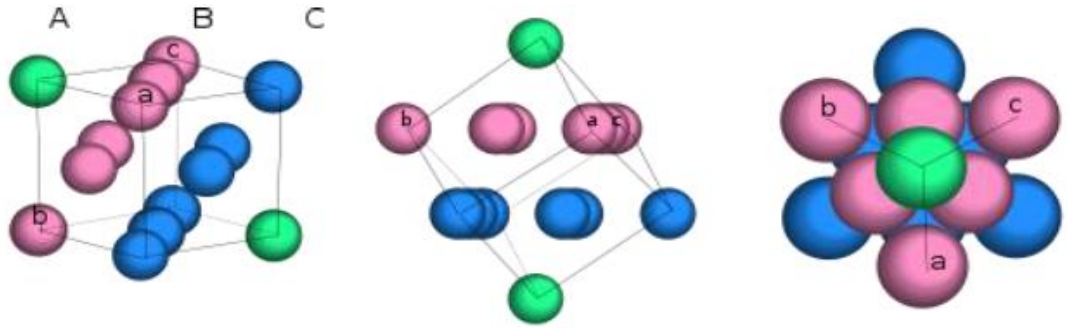

Figure I.8 A break down of cubic closest packing **[8]**

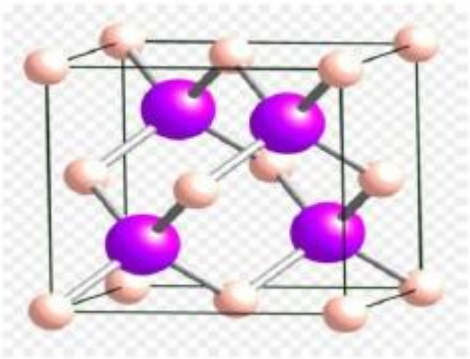

Figure I.9 A representation of ccp structure **[8]**

I.3.2 Electronic properties

The quantum theory of solids, which initially takes place within the framework of approximation to an electron, therefore establishes that the electronic states therein are grouped into bands, which opposes them to atoms. In these bands, the various states are distinguished by a vector of wave k, assimilable to the kinetic moment. In a semiconductor or insulator, the last populated strip (valence band, VB) is completely populated, resulting in the Pauli principle, that there is no place for a change of state, therefore a change of moment such as acceleration caused by an electric field. As for the first band empty (conduction band, CB), it is also completely empty, and therefore, there is nothing to accelerate. The temperature, or optical excitation by photons of energy greater than the gap, activating the promotion of electrons from VB to CB, change in principle this blocking situation electric. But it is above all doping with electrically active impurities which is of immense practical importance **[3]**.

III-V semiconductor materials have eight electrons per unit cell contributing to chemical bonds. The other electrons do not intervene in the optical properties of heterostructures. The orbitals of type s and type p of each atom (as an example the gallium Ga hybridize with the orbitals of the

arsenide atoms As), and form tetrahedral covalent bonds of type sp^3: 4 orbital binders and 4 antennae orbitals. The four orbital binders give rise to four energy bands, each degenerated twice of spin, and form the valence band.

This band is fully occupied by electrons with T=0K, for a perfect semiconductor. The other four antennae orbitals give rise to four upper bands, and form the conduction band which is unoccupied and separated from the previous one by a band of forbidden energy of width Eg (band gap). For direct gap semiconductors, the maximum of the valence band and the minimum of the conduction band are at point Γ.

I.3.2.1 Electronic energy band structure

The energy bands give the possible energy states for the electrons as a function of their wave vector. They are thus represented in the reciprocal space and to simplify, in the higher symmetrical directions of the first Brillouin zone. They break down into valence bands and conduction bands (**Figure I.10**). It is the lowest valence band, the highest conduction band, and the forbidden band that separates them that mainly determine the transport properties of the semiconductor **.**

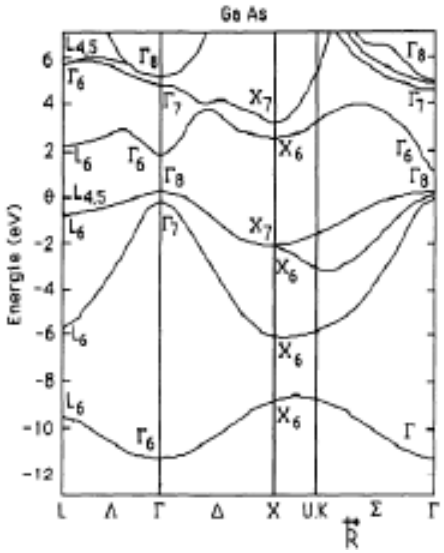

Figure I.10 Crystal structure of the GaAs **[9]**

I.3.2.2 Gap direct – Gap indirect

Consider the spread of different semiconductors. Deviation is by definition the width of the band gap, that is, the difference in energy between the absolute minimum of the conductivity and the

absolute maximum of the valence band. The band structure shown in Figure (1.11) shows two basic semiconductor cases.

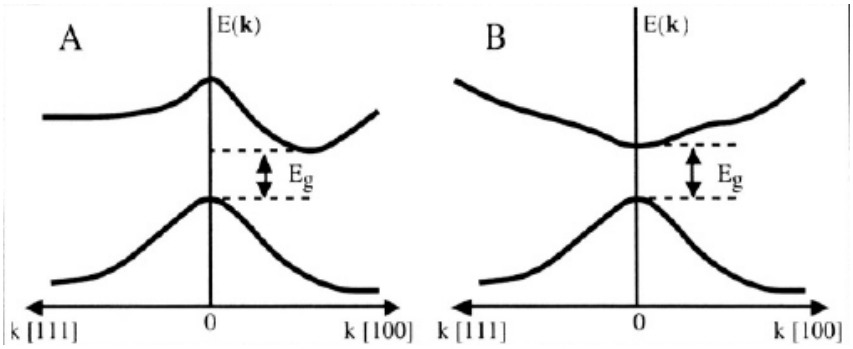

Figure I.11 Structure de bande d'énergie du : A-gap indirect et B-gap direct **[9]**

An indirect gap semiconductor, where the conduction band minimum and the valence band maximum are at different points in k space, and a direct gap semiconductor where these extremes are at the same point. a point in space k (in the center of the Brillouin region, at k=0).

In direct gab semiconductors, of which the minimal of the conduction band and the most of the valence band are positioned at specific factors withinside the k-area and direct hole semiconductors for which those extremes are positioned on the identical factor withinside the k-area (withinside the centre of the Brillouin area, in k=0) **[9]** .

I.3.3 Optical properties

The optical properties of semiconductors are closely related to their electronic structure in that they involve transitions between different electronic states.

The interaction of an electron with a photon, like any interaction, with conservation of energy and wave vectors. Since the wave vector of the photon is much smaller than the wave vector of the electron, direct optical transitions between the valence and conduction bands appear vertically in the electron band diagram. In the case of indirect closed-band semiconductors, the optical transition in space can only take place by an additional interaction, such as a phonon.

Semiconductors with indirect band inhibitors like GaP are very poor emitters and that is why silicon, which has been so successful in microelectronics, is not a good material for optoelectronics.

On the other hand, a direct band material such as GaAs, where the electrons and holes are on the maxima of their respective bands that are both at the point k=0 (see Fig.I-12) **[9]**.

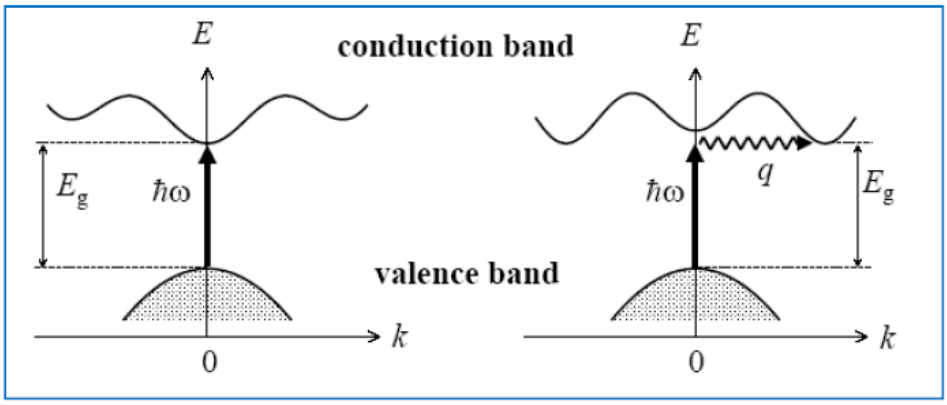

Figure I.12 direct and indirect optical transitions **[9]**

The optical characteristics of the materials are:

a. index of refraction

The index of refraction is a number that characterizes a material's ability to slow down and deflect light. This refractive index (n) is the ratio between the speed of light in a vacuum (c= 3×10^8 km/s) and the speed of light in the material, the refractive index can be expressed as a complex as a series **[10]**:

$$N(\omega) = n(\omega) + ik(\omega) \qquad \textbf{I.1}$$

$n(\omega)$: Being the real refractive index.

$ik(\omega)$: Is the attenuation index also called extinction coefficient.

The refractive index (**n**) of a semiconductor is a very important physical parameter related to micro-atomic interactions, it is often related to the gap energy.

Several methods have been considered for tuning the band gap of semiconductors with respect to their refractive index.

The correlation between **n** and **Eg** is important for the band structure of semiconductors, it is useful to find an acceptable n value of any material from this relationship.

There are several models to calculate this parameter, "**Moss**" was the first to find a relationship between the refractive index n and the energy gap Eg based on the atomic model, his formula is given as follows:

1) **Ravindra and Srivastava model:**

$$n^4 E_g = K \qquad \text{I-2}$$

Where the constant k=108eV is established by Ravindra and Srivastava **[11].**

2) Model of Gupta and Ravindra:

Linear form of Gupta and Ravindra :

$$n = \alpha + \beta E_g \qquad \text{I-3}$$

$\alpha = 4.084$ and $\beta = -0.62\ eV^{-1}$ [12]

3) Model by Herve-Vandamme:

The empirical relation of Herve and Vandamme given by :

$$n = \sqrt{1 + \left(\frac{A}{E_g + B}\right)^2} \qquad \text{I-4}$$

With A=13.6 eV and B=3.4 eV **[13]**

4) Model of Reddy and Anjaneyulu:

Reddy and Anjaneyulu's relationship :

$$E_g e^n = 36.6 \quad [14] \qquad \text{I-5}$$

5) Ravindra's Model :

linear form of Ravindra:

$$n = \alpha + \beta E_g \qquad \text{I-6}$$

α and β are constants with α=4.16 eV and β=-0.85 eV^{-1} [15]

A major problem with light-emitting diodes is the movement of light from inside the material to the outside. Indeed, once a photon is emitted, it is not certain that it leaves the semiconductor: because of its strong index, the internal total internal reflection angle is weak: it is close to 17 for GaAs, i.e. only 2% of total solid angle allows photons to exit the semiconductor from one side. As a result, many photons are reflected inward and eventually reabsorbed.

The huge commercial stakes surrounding light-emitting diodes (LEDs) today have spurred a whole community to search for the ideal optical structure for emitting light from a diode: anti-reflective mirror, micro cavity, pyramid, structure with photonic band gap. .. The problem is not simple at all.

I.4. The theory of alloys

An alloy is a homogeneous mixture of two or more materials. In an alloy, voluntarily added elements are referred to as "alloying or addition elements" and unwanted elements are referred to as "impurities". The evolution of modern techniques of crystalline growth and purification of semiconductors, allowed the creation of several binary, ternary and quaternary alloys. The application of these alloys in the fields of optoelectronics of microelectronics has prompted researchers to develop both theoretical and experimental aspects.

Alloy classification:

Semiconductor alloys are classified into several groups according to the number of constituents:

- **binary alloy:**

  Of the form AB: AII BVI : BeTe, MgTe.

- **ternary alloy:**

  When binary elements AB and AC are associated, the formed alloy can be:

  - cationic ternary alloy:A_xB_{1-x}C
  - anionic alloy : AB_xC_{1-x}

A ternary alloy is characterized by the x stoichiometric coefficient, this parameter allows to continuously vary the properties of the material, in particular the gap and the crystalline parameter.

- **Fourth alloy:**

  It is also possible to develop quaternary compounds consisting of four binary elements. These alloys can be either:

  - Quadratic solutions of the form : $A_{1-x}B_xC_yD_{1-x}$
  - Triangular solutions divided into two classes:
    - Des solutions purement anioniques : $AB_xC_yD_{1-x-y}$
    - Purely cationic solutions : $A_xB_yC_{1-x-y}D$

The advantage of quaternary alloys compared to binary and ternary alloys lies in the possibility to adjust almost independently their mesh parameter and the forbidden band energy by varying the two compositions x and y. It is therefore theoretically easy to obtain the desired forbidden band energy while maintaining mesh agreement with the substrate **[16]**.

I.4.1 The theory of ternary alloys

Alloy means a homogeneous mixture of two or more materials. There was a time when the word alloy was reserved only for metals, however this definition quickly became associated with other materials, especially ceramics and polymers.

Shortly after the development of modern crystalline growth techniques and the purification of semiconductors, several binary, ternary and quaternary alloys were made.

The use of the latter in the fields of microelectronics and optoelectronics encouraged researchers to develop the theoretical as well as the experimental side.
Indeed, the development made via way of means of chemists, fabric physicists and technologists has contributed correctly to the have a look at and manufacture of latest substances amongst them semiconductor alloys III-V and II-VI **[17].**

The practical value of III-V semiconductors is further considerably enhanced by the possibility of making alloys by partial substitution of one element by another element of the same column. For example, ternary or quaternary alloys are known to be identified as follows:
Ternary: If there is substitution of 2 atoms on one of the subarrays, that is, $A_xA'_{(1-x)}B$.
Example: $Ga_xIn_{(1-x)}P$ when the exact composition counts little, we write short GaInP **[6]**.
III-V semiconductors are of great interest because of their properties **[7]** :

- They are sturdy.
- They have high thermal conductivity.
- Their merger points are high.
- They have a direct or indirect prohibited band.

I.4.2 The theory of a ternary semiconductor alloy $Al_xGa_{1-x}As$

AlGaAs is the most important and most studied III-V semiconductor alloy. Its key role in a wide variety of transistors and optoelectronic devices requires precise knowledge of the fundamental bandgap as well as the alignment of the three main conduction band depressions. Investigations are complicated by the fact that GaAs is a direct pore material with the G–L–X valley order. AlAs is an indirect material with reverse order. Special attention is paid to the intersection, at which valley minima G and X have the same energy.

Bowing parameters for the *X*-valley and *L*-valley gaps in AlGaAs were determined using electrical measurements in combination with a theoretical model by Lee *et al.* and Saxena as well

as empirically by Casey and Panish. These results and photoluminescence excitation spectroscopy data support a $C(E_g^L)$ almost equal to zero. We select $C(E_g^X)$ =0.055eV obtained from photoluminescence measurements, which is near the bottom of the earlier range of values but is the most recent and seems the most reliable. This result implies a $\Gamma - X$ crossover composition of x=0.38 at low temperatures (and 0.39 at 300 K), which agrees with the trend in the table compiled by Adachi. Composition dependences for all three of the direct and indirect gaps in $\mathbf{Al_xGa_{1-x}As}$ are plotted in **Fig 1.8** . Most studies find that the split-off gap can be fit quite well by linear interpolation. A value of $C(\Delta_S) = 0.147$ eV derived by Aubel *et al.* cannot be considered fully reliable, since it was based on data points in a rather narrow composition range.

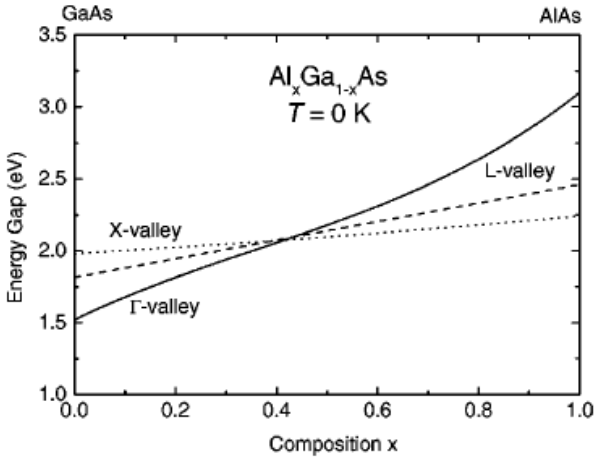

Figure I.8: Γ -, *X*-, and *L*-valley gaps for the AlGaAs alloy at *T* = 0 K (solid, dotted, and dashed curves, respectively) **[2]** .

Several studies of the composition dependence of the G-valley electron mass have been reported for $x < 0.33$. The points have been fit to a quadratic dependence, although owing to the narrow composition range and spread in the data points, it is difficult to judge the accuracy of such a scheme. From other reports, it appears that the linear approximation gives adequate results for small *x*. Since the effective mass in AlAs was chosen to be consistent with the results in AlGaAs, a zero bowing parameter is recommended and gives good agreement with the interpolation procedures discussed at the beginning of Sec. V. The same procedures should be used to obtain the *X*-valley and *L*-valley electron masses, Luttinger parameters, and hole masses **[2]**.

I.4.3 Virtual Crystal Approximation (VCA)

For all of the ternary alloys discussed below, the dependence of the energy gap on alloy composition is assumed to fit a simple quadratic form **[2]**:

$$E_g(A_{1-x}B_x) = (1-x)E_g(A) + xE_g(B) - x(1-x)C \qquad \textbf{I-7}$$

In the Virtual-Crystal Approximation (VCA), it is assumed that alloys composed of certain types of atoms A and B are, for example, randomly distributed over the positions of the lattice. The representative potential of the alloy per site is considered as a superposition of the atomic potentials of each type A and B proportional to their concentration in mathematical terms.

$$V_{VCA} = xV_A + (1-x)V_B \qquad \textbf{I-8}$$

Where x is the atomic concentration of atom type A and VA, VB is the atomic potential energy of atoms A, B, respectively. Therefore, we construct an effective Hamiltonian where the potential is replaced by V_{eff}. Thus, these Hamiltonian eigenvalues and eigenvectors represent a completely disordered alloy **[18]**.

I.5. Technological benefits of semiconductor alloys

Of all the possible binary compounds, not all have the same potential benefits. Studying their properties, and especially the structure of the bands, shows that the lightest elements form compounds with wide band gap, whose properties closely resemble those of insulators. Compounds consisting of boron, aluminum or nitrogen, and gallium phosphide fall into this category, which are generally of little interest for fast electronic devices requiring semiconductors with high carrier mobility or for optoelectronics where A direct band structure is required for efficient optical conversion. On the other end, heavy elements like thallium or bismuth etc. metal compounds are formed. Therefore, we will basically consider compounds based on gallium (GaAs, GaSb) or aluminum (AlAs, AlN), which have the most interesting properties.

III-V semiconductors are of great importance today, both in research and industry.

Conclusion:

In this part we learned about the generalities of semiconductors and showed us their physical, quantitative, electrical and optical properties, as well as the composite semiconductors and ternary such as AlGaAs which has many photovoltaic and electrical properties because of its physical and quantitative composition.

Chapter II

Methods for calculating energy bands

II.1 Introduction

Methods for calculating energy bands, also known as band structure calculations, play a crucial role in understanding the electronic properties of materials. These calculations provide valuable insights into the behavior of electrons and their energy levels within solids.

Each method has its strengths and limitations, and the choice of method depends on factors such as the properties of the material, computational resources available, and desired level of accuracy. Band structure calculations provide essential insights into the electronic properties of materials, aiding in the design and optimization of various electronic and optoelectronic devices. They contribute to advancing our understanding of materials and enable the development of innovative technologies.

These methods, along with various approximations and numerical techniques, allow scientists to compute the energy bands of electrons in solid materials, providing valuable insights into their electronic properties and behavior.

Knowledge of electronic structure plays a key role in understanding the physical and chemical properties of materials. Computing the electronic structure of a crystal is like solving the problem of interactions between many nuclei and electrons, making it impossible to solve the Schrödinger equation.

II.2 Equation of Schrödinger

Schrodinger's equation is the fundamental equation of quantum physics, like Newton's laws in classical physics. We find it to write phenomenal more varied whether in atomic physics, quantum optics, plasma physics, chemistry or biology .... The Schrodinger equation was inductively proposed by the physicist Erwin Schrodinger in 1926, and developed first with the aim of writing the small objects (atoms) made up of a single particle located in a certain force field (the electron within the hydrogen atom, for example). A complete description of a quantum system with N electrons requires the calculation of the corresponding wave function: $\boldsymbol{\psi(r_1, \dots, r_i, \dots, r_N)}$, $\boldsymbol{r_i}$represents the position of each electron i. In principle, this can be obtained from the time-independent Schrodinger equation:

$$\boldsymbol{H\psi = E\psi} \qquad \textbf{(II.1)}$$

where H is the hamiltonian of the interacting electron system in an external potential $V_{ext}(r)$, **E** is the electronic energy and $\boldsymbol{\psi}$ is the wave function. The total non-relativist Hamiltonian operator can be expressed more precisely by:

$$\hat{H} = \hat{T}_{noy} + \hat{T}_{el} + \hat{V}_{el-noy} + \hat{V}_{el-el} + \hat{V}_{noy-noy} \quad \textbf{(II.2)}$$

with:

$$\hat{T}_{noy} = -\frac{\hbar^2}{2}\sum_i \frac{\nabla_i^2}{M_n} \quad \textbf{(II.3)}$$

is the kinetic energy of the M nuclei M_n mass and $\vec{R}_i$ position.

$$\hat{T}_{el} = -\frac{\hbar^2}{2}\sum_i \frac{\nabla_i^2}{m_e} \quad \textbf{(II.4)}$$

is the kinetic energy of the N electrons of mass m_e and position $\vec{r}_i$.

$$\hat{V}_{noy-el} = -\frac{1}{4\pi\varepsilon_0}\sum_{i,j}\frac{e^2 Z_i}{|\vec{R}_i - \vec{r}_j|} \quad \textbf{(II.5)}$$

is the attractive coulombian nucleus-electron interaction, **Z** indicates the atomic number and **e** electron charge.

$$\hat{V}_{el-el} = \frac{1}{8\pi\varepsilon_0}\sum_{i\neq j}\frac{e^2}{|\vec{r}_i - \vec{r}_j|} \quad \textbf{(II.6)}$$

is the electron-electron repulsive coulombian interaction.

$$\hat{V}_{noy-noy} = \frac{1}{8\pi\varepsilon_0}\sum_{i\neq j}\frac{e^2 Z_i Z_j}{|\vec{R}_i - \vec{R}_j|} \quad \textbf{(II.7)}$$

is the Coulomb repulsive nucleus-nucleus interaction.

The exact expression of the Hamiltonian system is therefore:

$$\hat{H} = -\frac{\hbar^2}{2}\sum_i \frac{\nabla_i^2}{M_e} - \frac{\hbar^2}{2}\sum_i \frac{\nabla_i^2}{m_e} - \frac{1}{4\pi\varepsilon_0}\sum_{i,j}\frac{e^2 Z_i}{|\vec{R}_i - \vec{r}_j|} + \frac{1}{8\pi\varepsilon_0}\sum_{i\neq j}\frac{e^2}{|\vec{r}_i - \vec{r}_j|} + \frac{1}{8\pi\varepsilon_0}\sum_{i\neq j}\frac{e^2 Z_i Z_j}{|\vec{R}_i - \vec{R}_j|} \quad \textbf{(II.8)}$$

Dealing with the many-body problem in quantum mechanics, including solving the exact Schrödinger equation where the overall wavefunction depends on the 3N coordinates of all particles, is an extremely difficult, if not desirable, task. say impossible, because numerical systems have no method of solving problems when the number of variables is as large as in the atomic system **[20]**.

Solids are formed by the binding of elementary particles: nuclei and electrons interact. The fundamental theoretical problem of solid-state physics is to understand the organization of these particles at the origin of their properties. But in this case, classical mechanics proved insufficient and it was necessary to resort to quantum mechanics, the basis of which was the solution of the Schrödinger equation proposed by the Austrian physicist Erwin Schrödinger in 1926 describing all the this interaction.

$$\boldsymbol{H\psi = E\psi} \quad \textbf{(II.9)}$$

The problem of solving the Schrödinger equation is reduced to the problem of the behavior of electrons, but it is still very complicated by the existence of an electron-electron interaction term (the last term of the equation). The difficulty of describing these interacting electrons requires the use of approximations to solve this problem, such as the Hartree approximation we explain below. **[21]**.

II.3 Approximations

II.3.1 Born-Oppenheimer approximation

This approximation is based on the fact that the mass of the nucleus is significantly greater than the mass of the electron. For this reason it is possible to ignore the motion of the nuclei with respect to the electrons, i.e. the nuclei will be considered classified, we take the example of the mass of a hydrogen nucleus which is 3672 times greater. the mass of the electron, for example for carbon, this ratio and 22032 times. However, we can consider that electrons are moving in the field created by the nuclei. This is the Born-Oppenheimer approximation. This means that the first term of the previously written Hamiltonian (nuclear kinetic energy) can be ignored and the fifth term (Coulombian nuclear-nuclear interaction) is just a constant. Equation (**II.8**) becomes:

$$\hat{H} = -\frac{\hbar^2}{2}\sum_i \frac{\nabla_i^2}{M_e} - \frac{\hbar^2}{2}\sum_i \frac{\nabla_i^2}{m_e} - \frac{1}{4\pi\varepsilon_0}\sum_{i,j}\frac{e^2 Z_i}{|\vec{R}_i-\vec{r}_j|} + \frac{1}{8\pi\varepsilon_0}\sum_{i\neq j}\frac{e^2}{|\vec{r}_i-\vec{r}_j|} + \underbrace{\frac{1}{8\pi\varepsilon_0}\sum_{i\neq j}\frac{e^2 Z_i Z_j}{|\vec{R}_i-\vec{R}_j|}}_{\hat{C}^{ste}} \quad \textbf{(II.10)}$$

and with the use of atomic unity ($\hbar = e = m_e = 4\pi\varepsilon_0 = 1$), Hamiltonian thus becomes:

$$\hat{H} = \underbrace{-\frac{1}{2}\sum_i \nabla_i^2}_{\hat{T}} + \underbrace{\frac{1}{2}\sum_{i\neq j}\frac{1}{|\vec{r}_i-\vec{r}_j|}}_{\hat{V}} + \underbrace{\sum_{i,j}\frac{Z_i}{|\vec{R}_i-\vec{r}_j|} + C^{ste}}_{\hat{V}_{ext}} \quad \textbf{(II.11)}$$

As a result, the hamiltonian of the system is reduced in three terms: the kinetic energy of electrons $\hat{\boldsymbol{T}}$, the potential energy due to electron-electron $\hat{\boldsymbol{V}}$ interactions (which will be named after: the Hartree potential) and the external potential $\hat{\boldsymbol{V}}_{\boldsymbol{ext}}$ which represents both the potential for nucleus-nucleus interactions and those of other electron-nuclei in the system, we write:

$$\hat{\boldsymbol{H}} = \hat{\boldsymbol{T}} + \hat{\boldsymbol{V}} + \hat{\boldsymbol{V}}_{\boldsymbol{ext}} \quad \textbf{(II.12)}$$

However, the Born-Oppenheimer approximation still fails to solve the Schrodinger equation due to the correlation of the electron distribution interactions. Additional approximations are used, including that of Hartree **[10]**.

II.3.2 Hartree approximation

Hartree's model is based on a particular expression of solutions, in fact, we will assume that electrons are independent, this translates to:

$$(r1, r2, \dots rn) = \psi 1(r1)\psi 2(r2) \dots \psi(rn) \quad \textbf{(II.13)}$$

Where:
: Electron position **i** with i=1… n.

The Schrödinger equation to a single particle (electron) is given as follows:

$$Hi\psi i\,(r) = Ei\psi i\,(r) \quad \textbf{(II.14)}$$

With:

$$\widehat{H} = -\frac{\hbar^2}{2m}\Delta_i + V_{ext}(r) + V_i(r) \quad \textbf{(II.15)}$$

Where:

$V_{ext}(r)$: Potential for electron-nucleus interaction.
$V_i(r)$: Hartree's potential for the $\mathbf{i^{th}}$ electron, which has the form:

$$\widehat{V}_1(\mathrm{r}) = \frac{-\mathrm{e}\int \rho_i(\mathrm{r}')}{|\mathrm{r}-\mathrm{r}'|}\,\mathrm{d}^3\mathrm{r} \quad \textbf{(II.16)}$$

The density of electrons $\boldsymbol{\rho_i}\,(\mathbf{r}')$ being given by:

$$\rho_i = -e\sum_{\substack{j=1\\ x\neq j}}^{N_e}\left|\psi_j(r)\right|^2 \quad \textbf{(II.17)}$$

The sum is made on the $\mathbf{N_e}$ mono-electronic states.

Schrödinger's equation will take the form:

$$\left[-\frac{\hbar^2}{2m}\Delta_i - -e\sum_{\substack{j=1\\ x\neq j}}^{N_e}\int\frac{|\psi_j(r)|^2}{|\mathrm{r}-\mathrm{r}'|}\mathrm{d}^3\mathrm{r} + \widehat{V}_{ext}(r)\right]\psi_j(r) = E_i\psi_j(r) \quad \textbf{(II.18)}$$

Equation **II-18** is called the Hartree particle equation.

The disadvantage of this method is that it does not consider the anti-symmetry of the wave function **[21].**

II.3.3 Hartree-Fock approximation

Hartree's method allows to represent the overall wavefunction as a direct product of one-electron functions since the motion of the electrons is decoupled from the motion of the nucleus according to the Born Oppenheimer approximation, and the electron wavefunction is written :

$$\boldsymbol{\psi}(\vec{\boldsymbol{r}}_1, \vec{\boldsymbol{r}}_2, \vec{\boldsymbol{r}}_3, \dots, \vec{\boldsymbol{r}}_N) = \boldsymbol{\psi}_1(\vec{\boldsymbol{r}}_1).\boldsymbol{\psi}_2(\vec{\boldsymbol{r}}_1).\boldsymbol{\psi}_3(\vec{\boldsymbol{r}}_1)\dots\boldsymbol{\psi}_N(\vec{\boldsymbol{r}}_1) \qquad (\mathbf{II.19})$$

In 1930, Fock showed that Hamilton solutions (II.11) violate the Pauli exclusion principle because they are not antisymmetric to the exchange of any two electrons.

The antisymmetric of the electron wave function is written, by exchanging two electrons, for example:

$$\boldsymbol{\psi}(\vec{\boldsymbol{r}}_1, \vec{\boldsymbol{r}}_2, \dots, \vec{\boldsymbol{r}}_i, \dots, \vec{\boldsymbol{r}}_j \dots, \vec{\boldsymbol{r}}_N) = -\boldsymbol{\psi}(\vec{\boldsymbol{r}}_1, \vec{\boldsymbol{r}}_2, \dots, \vec{\boldsymbol{r}}_i, \dots, \vec{\boldsymbol{r}}_j \dots, \vec{\boldsymbol{r}}_N) \qquad (\mathbf{II.20})$$

Thus, such a description follows the Pauli exclusion principle imposed on two electrons, having the same quantum number, which cannot simultaneously occupy the same quantum state, nor the indistinguishability of the electrons. But in Hartree's wavefunction formula, this is not the case, because electron **i** occupies exactly state **i**. Hartree and Fock generalized this concept by showing that Pauli's principle is satisfied if one writes the wave function in terms of Slater's determinant:

$$\psi(\vec{r}_1\vec{\sigma}_1, \vec{r}_2\vec{\sigma}_2, \dots, \vec{r}_N\vec{\sigma}_N) = \frac{1}{\sqrt{N!}} \begin{vmatrix} \psi_1(\vec{r}_1\vec{\sigma}_1) & \psi_1(\vec{r}_2\vec{\sigma}_2) & \dots & \psi_1(\vec{r}_N\vec{\sigma}_N) \\ \psi_2(\vec{r}_1\vec{\sigma}_1) & \psi_2(\vec{r}_2\vec{\sigma}_2) & \dots & \psi_2(\vec{r}_N\vec{\sigma}_N) \\ \dots & \dots & \dots & \dots \\ \psi_N(\vec{r}_1\vec{\sigma}_1) & \psi_N(\vec{r}_2\vec{\sigma}_2) & \dots & \psi_N(\vec{r}_N\vec{\sigma}_N) \end{vmatrix} \qquad \mathbf{(II.21)}$$

- where $\vec{\boldsymbol{\sigma}}$ represents the spin **[19]**.

This system of equations is solved automatically insofar as the potential energy depends on the functions of the wave, which is difficult to solve by numerical analysis techniques when the system under study consists of a large number of solid-like electrons. , but it is still a starting point, either to perform additional approximations as in the case of semi-empirical methods, or to add additional determinants that produce solutions that converge to a single solution. method as close as possible to the exact solution of the electronic Schrödinger equation.

It should also be noted that, according to the Hartree-Fock method, electrons are considered to be independent of each other and each electron moves in an average potential created by all the nuclei and other electrons. The exchange term is treated exactly according to this approximation, while electron correlation (or instantaneous repulsion between electrons) is ignored. Fraudulent methods later appeared (such as: Post-Hartree-Fock, Moller-Plesset Disturbance Theory, Setup Interaction, Coupled cluster method, etc.), but all these methods are derived from the Hartree-Fock method. are not taken into account. are only part of the correlation energy and are aimed at small systems because they are computationally expensive.

II.4.The pseudopotential method

The pseudopotential method, like the OPW method, uses the orthogonality of the valence and conduction states to the cardiac states. But in the pseudopotential form, the orthogonal effect is introduced into the potential energy in the form of an equivalent potential energy called the pseudopotential.

Orthogonality in core states has the effect of extracting from the crystal potential the rapidly changing contribution of the core region. The pseudo-potential then changes gradually and is consistent with a perturbation approach to the problem.

The pseudopotential theory was introduced by Fermi in 1934 in his work on thin film states. Years later, Helmand proposed a pseudopotential method to calculate the energy levels in alkali metals. And it was in 1950 that this theory expanded into a quick report on energy calculations and other properties of semiconductors.

The calculation is based on the orthogonal plane wave (OPW) method. The basic idea of this method is to obtain the valence states of an "atom, molecule, crystal". without resorting to computations of core states that are not necessary for the description of physical properties. The electrons in the nucleus will be considered frozen and only valence electrons move in a potential. The coefficients used in the OPW method to ensure the plane wave orthogonality to the cardiac states help to produce a push potential and a weak or pseudopotential that is obtained by the suppression effect. This method is used to calculate the electronic structure of solids and liquids, lattice vibrations, bonds and the structure of crystals, ... etc **[21]** .

II.5.The empirical method of pseudo potential (EPM)

Experimental pseudopotential method (EPM) has been widely and successfully applied in some semiconductors with mixed diamond or zinc structures. Here is an approach to calculate the form factors of the pseudopotential. In this approximation, X-ray and UV reflection and photoluminescence experiments play a very important role in determining the parameters used in the band structure calculation.

II.5.1 Local empirical method

This approach (EPM) solves the problem of adjusting the experimental form factors V(G) of the pseudopotential Vps which can be written in the reciprocal network in the form:

$$V_{ps}(r) = \sum_g V(g) \exp(ig.r) \quad \textbf{(II.22)}$$

Whith

$$V_{ps}(r) = \sum_a S_a(g) \times V_a(g) \quad \textbf{(II.23)}$$

g : Vector of reciprocal network.

$\boldsymbol{V_\alpha}$**(g)** : form factor associated with latoma α .

$\boldsymbol{S_\alpha}$**(g)** : atomic structure factor provided by:

$$V_{ps}(r) = \frac{1}{N_a} \exp(ig.r_{ia}) \quad \textbf{(II.24)}$$

$\mathbf{N_\alpha}$: number of atoms.

$\mathbf{r_{i\,\alpha}}$: position of i^{th} type atom α.

In the case of a zinc blende structure, for example, there are two atoms A and B:

$\mathbf{r_A}$ (0, 0,0) a and $\mathbf{r_B}$ (1/4,1/4,1/4) a (a is the network parameter), shape and structure factors are written:

$$V(g) = S_A(g)V_A(g) + V_B(g)S_B(g) \quad \textbf{(II.25)}$$

Whith :

$$S_A(g) = \frac{1}{2} e^{-igr_A} \quad \textbf{(II.26)}$$

$$S_B(g) = \frac{1}{2} e^{-igr_B} \qquad \textbf{(II.27)}$$

Taking the origin in the middle of the line that joins the two atoms A and B

$$r_A = \frac{a}{8}(1,1,1) = -r_B = S \qquad \textbf{(II.28)}$$

is obtained

$$V(g) = e^{-igS} V_A(g) + V_B(g) e^{igS} \qquad \textbf{(II.29)}$$

The symmetric form factors $\mathbf{V_S}$ and antisymmetric $\mathbf{V_A}$ are defined by:

$$V^S(g) = \frac{1}{2}[V_A(g) + V_B(g)] \qquad \textbf{(II.30)}$$

$$V^A(g) = \frac{1}{2}[V_A(g) - V_B(g)] \qquad \textbf{(II.31)}$$

$$V_{ps}(r) = V^S(g)\cos(gS) + V^A(g)\sin(gS) \qquad \textbf{(II.32)}$$

The E.P.M calculation method as shown in the following diagram is selected (G). The structure is included by the structure coefficient and the Schrödinger equation is solved for the energy eigenvalues E(k) and pseudo wavefunctions ψk(r).

These energies are compared with experiment and V(G) is changed if a good agreement between experiment and theory is not achieved. This process is repeated until a good agreement between experiment and theory is reached. A small number of iterative steps is usually sufficient to fit theory and experiment.

The procedure to compute the E.P.M method is illustrated in the following diagram:

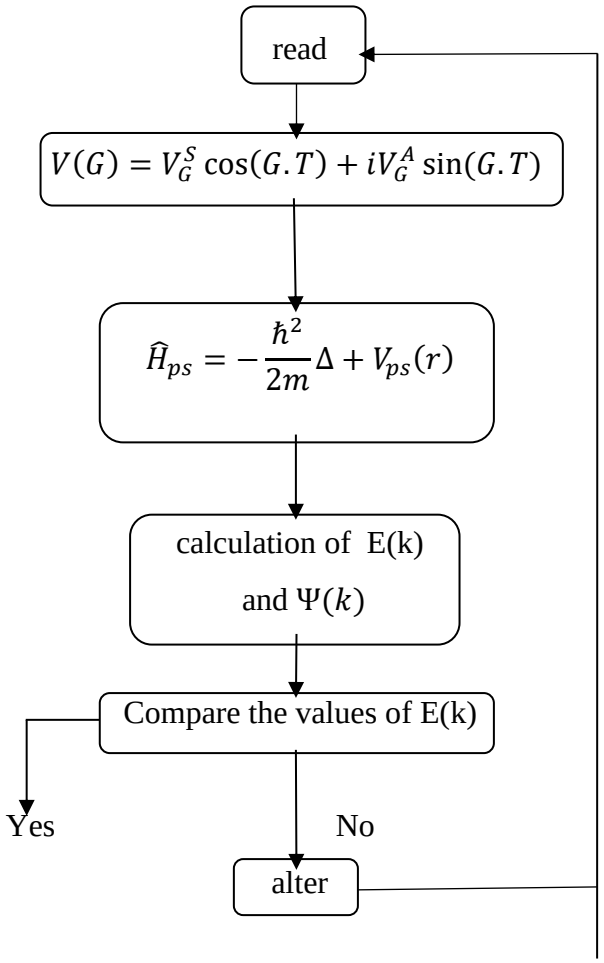

Figure II.1. The local empirical pseudopotential approach.

Conclusion

The pseudopotential method is currently the most widely used method for determining the electronic band structure and other properties such as band gap.

The choice of empirical pseudo-potentials (EPM) method is basically based on the fact that the valence states are obtained without calculating core states that are not necessary for the description of the physical properties of a system. Real states are described by pseudo-wave functions that are represented in Fourier space by a limited number of plane waves, thus minimizing numerical calculations.

We have proposed a method to calculate the energy band structure of these materials.

Chapter III

results and discussions

III.1 Introduction

In semiconductors, two fundamental properties, namely band gap and refractive index, mainly determine their optical and electronic behavior. The refractive index of a material usually decreases with increasing band gap promoting a fundamental relationship between these two fundamental quantities **[22]**.

At present, multi-component alloys have attracted much attention due to their use as substrates, coatings, active elements in optoelectronic devices of high-speed photonic devices and for other applications. The device performance characteristics depend on the electronic properties of the constituent materials, which can be improved by the use of tertiary alloys. Therefore, ternary alloys are widely used materials in the production of electronic components. Knowledge of these properties is necessary to define their field of application.

Through the above, we will study the optoelectronic properties of the $Al_XGa_{1-X}As$ triplet by numerical simulation, We chose the empirical pseudo-potential method (EPM) combined with virtual crystal approximation (VCA). and we performed these calculations on our GaAs and AlAs binaries.

III.2 Study of electronic properties

The calculations are mainly based on the experimental pseudopotential method (EPM) with the use of virtual crystal approximation (VCA) improved according to the structural model of the zinc blende. Ignore the effects of the disorder.

In EPM, the crystal potential is expressed as a linear superposition of the atomic potentials modified and adjusted to have the same value of the known band gap at selected points in the Brillouin region.

To know the following parameters (gap band structure, band gap, refractive index and high frequency dielectric constant), it is first necessary to study and determine the electronic and optical properties of the ternary semiconductor alloy $\mathrm{Al_xGa_{(1-x)}As}$.

The empirical nature of the pseudo-potential method consists in adjusting the form factors, in order to achieve the closest agreement of the calculated energy levels with the theoretical values. **[23]**

The parameters of the empirical pseudo potential V(G):

- are determined by the nonlinear least squares method.
- all parameters are optimized simultaneously according to a well-defined criterion to minimize the mean square root of the recorded deviation difference (rms).

III.2.1 variation of Gap energy as a function of X

Form factor values are taken at the start to be improved or modified by iterating until minimized **[24]**.

The form factors of the semiconductor binary compounds GaAs and AlAs are fitted and illustrated in Table (**III-1**).

III.2.1.1 The form factors

In the present study, the optoelectronic properties of the ternary alloy $Al_XGa_{1-X}As$ deposited on two binary GaAs and AlAs substrates are investigated.

The symmetric VS and adjusted VA pseudo-potential form factors and the network parameters of the binary compounds used are given in the table (**III-1**)

Table III-1 Pseudopotential form factors of GaAs, AlAs compounds.

The binary compound	**The form factors**						The constants of the network
	Vs(3)	Vs(8)	Vs(11)	Va(3)	Va(4)	Va(11)	a(A^0)
GaAs	-0.239833	0.0126	0.059625	0.060536	0.05	0.01	5.653
AlAs	-0.212694	0.00	0.09275	0.068833	0.05	-0.0075	5.6611

By including potential pseudo-parameters in the EPM code and their values mentioned in Table (III.1), we see the energy difference illustrated in Table (III.2) and very consistent with the experience reported by reference **[2]**.

III.2.2 Energy gap for $Al_XGa_{1-X}As$ alloy

Variation of direct energy difference E_Γ^Γ and indirect energy E_X^Γ , E_L^Γ have been calculated For the different x components of InxGa1-xSb ranging from 0 to 1, our results are presented in the table. (III-2).

Table III-2 Calculated and Experimental value band gap Energies gaps for the binary compounds (GaAs and ALAs)

components	E_{Γ}^{Γ}(eV)	E_{X}^{Γ}(eV)	E_{L}^{Γ}(eV)
GaAs	1.42118 [a)] 1.420 [b)]	1.81424 [a)] 1.981[b)]	1.72264 [a)] 1.815 [b)]
AlAs	2.9513 [a)] 2.9 [b)]	2.14773 [a)] 2.23 [b)]	2.36258 [a)] 2.35 [b)]

Where:

[a)]: calculated value.

[b)]: Experimental value in Ref **[2]**.

We found that our results were in better agreement with that reported by Ref **[2]**.

The variation of the fundamental gap (E_{Γ}^{Γ}) of the $Al_XGa_{1-X}As$ alloy as a function of the x composition is shown in the figure (III-1).

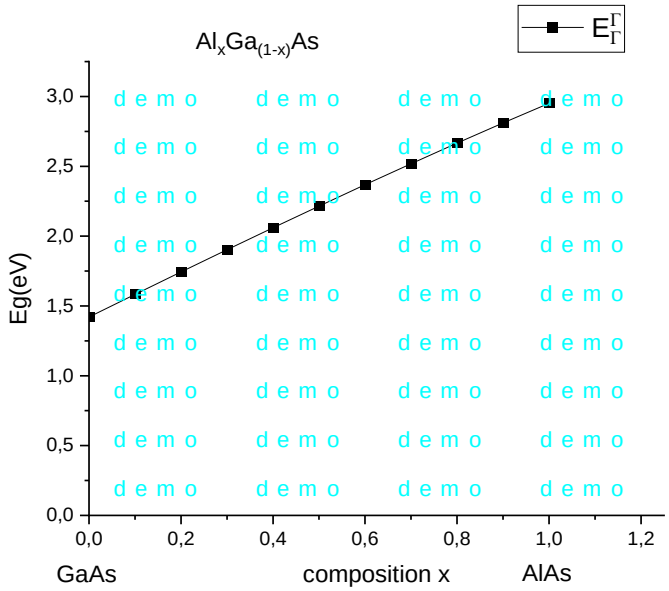

Figure III -1: The variation of the direct gap (E_{Γ}^{Γ}) of the $Al_XGa_{1-X}As$ Alloy as a function of the x composition.

The quadratic interpolation using the least squares method on the curve gives us the following analytic expression:

$$E_{\Gamma}^{\Gamma} = -0.11431x^2 + 1.64761x + 1.4197 \qquad \text{(VCA)} \qquad \textbf{(III-1)}$$

The curve shows that the variation is monotonic and increases from 1.42118 eV for GaAs to 2.9513 eV for AlAs.

The variation of the fundamental gap (E_X^{Γ}) of the $Al_XGa_{1-X}As$ alloy as a function of the x composition is shown in the figure (III-2).

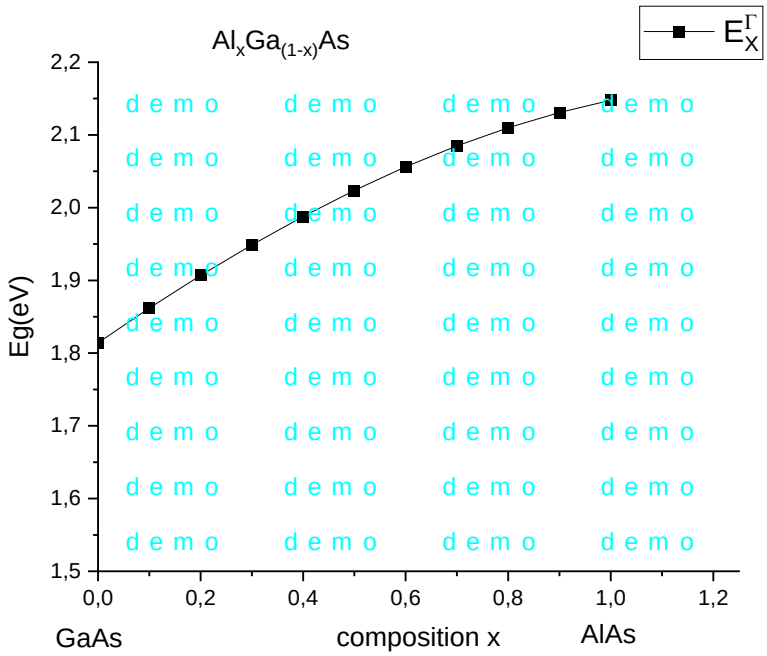

Figure III -2 The variation of the indirect gap (E_X^{Γ}) of the $Al_XGa_{1-X}As$ Alloy as a function of the x composition.

The quadratic interpolation using the least squares method on the curve gives us the following analytic expression:

$$E_X^{\Gamma} = -0.171\ x^2 + 0.50673\ x + 1.81315 \qquad \text{(VCA)} \qquad \textbf{(III-2)}$$

The curve shows that the variation is monotonic and decreases from 1.814224 eV for GaAs to 2.14773 eV for AlAs.

The variation of the fundamental gap (E_L^{Γ}) of the $Al_XGa_{1-X}As$ alloy as a function of the x composition is shown in the figure (III-3).

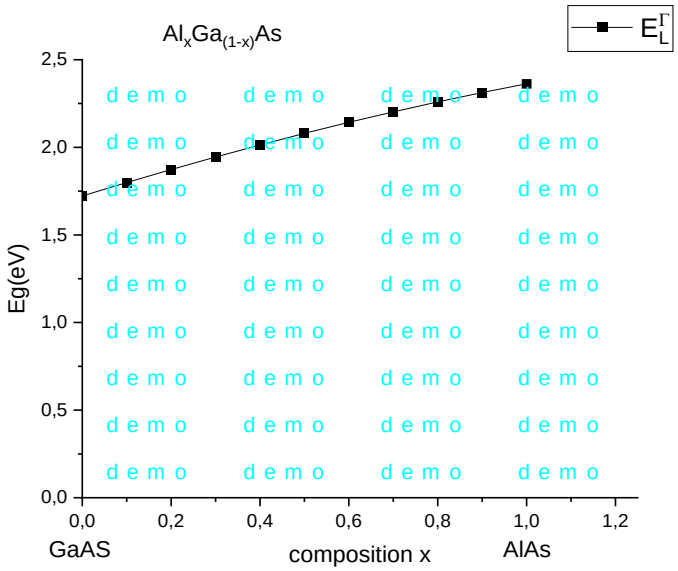

Figure III -3: The variation of the indirect gap (E_L^{Γ}) of the $Al_XGa_{1-X}As$ Alloy as a function of the x composition.

The quadratic interpolation using the least squares method on the curve gives us the following analytic expression:

$$E_L^{\Gamma} = -0.14739\,x^2 + 0.78895\,x - 0.14739 \qquad \textbf{(III -3)}$$

The curve shows that the variation is monotonic and decreases from 1.72264 eV for GaAs to 2.36258 eV for AlAs.

To see the possible transition of direct and indirect gap, figure (III -4) is drawn:

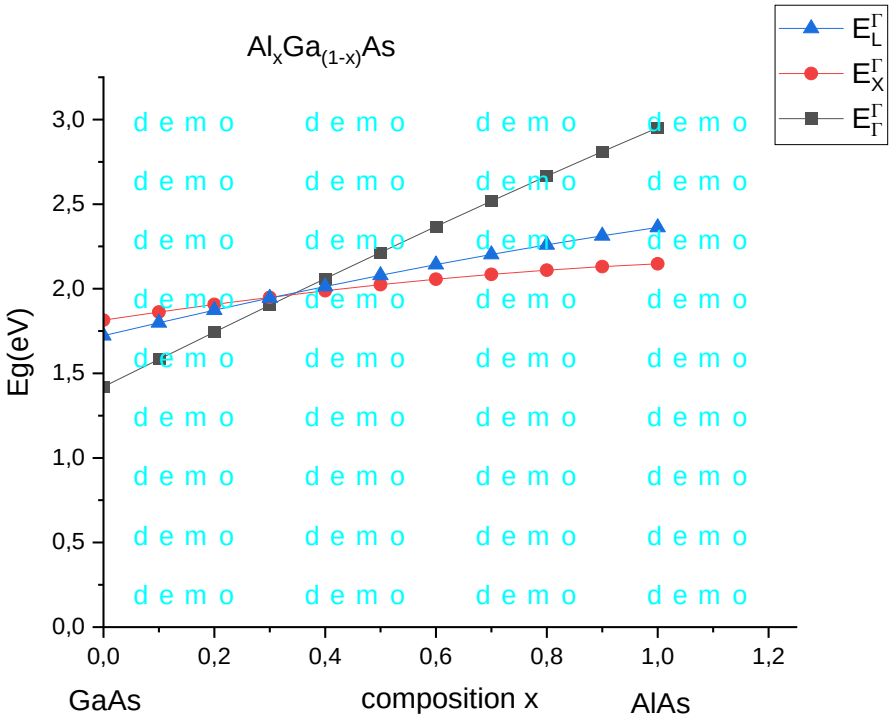

Figure III-4: The variation of the direct (E_Γ^Γ) gap and indirect gaps (E_X^Γ) (E_L^Γ) of the $Al_XGa_{1-X}As$ Alloy as a function of the x composition.

Through this curve, we see that the direct (E_Γ^Γ)and indirect (E_X^Γ) (E_L^Γ) gap is growing as the X composition increases, this variation is monotonous and linear.

The ternary alloy $Al_XGa_{1-X}As$ is a semiconductor with a direct gap (E_Γ^Γ) in the field from 0 to 0.3, and an indirect gap (E_X^Γ) in the field from 0.4 to 1 From the composition range x. This direct gap changes from 1.42118 for GaAs and 2.9513 for AlAs . The indirect gap changes from 1.81424 for GaAs and 2.14773 for AlAs . on Network parameter ranging from 5.653 a(Å) for GaAs to 5.6611 a(Å) for AlAs.

The results indicate that there are two band gaps namely direct and indirect gaps of the $Al_XGa_{1-X}As$ alloy for all compositions of x, leading to the conclusion that the alloy is a semiconductor with two gaps. The value of the direct gap ranges from 1.42118 to 1.9025 each time the transition varies from 0 to 0.3 of composition X, and the value of the indirect gap ranges from 1.98794 to 2.14773 each time the transition varies from 0.4 to 1 of composition X.

III.2.3 Lattice parameter

Vegard's law is an empirical rule stating that the property value of an alloy can be determined from linear interpolation of the property values of the elements. constituting it or in the case of higher alloys, the constituent Compounds **[25]**.

Vegard's law assumes that both components A and B in their pure form (i.e. before mixing) have the same crystal structure. Here, aAxB(1-x) is the lattice parameter of the solution, aA and aB are the lattice parameters of the pure components, and x is the mole fraction of B in the solution. The law is written in the following form:

$$aAB = axA + (1-x)axB \qquad \textbf{(III-4)}$$

For our alloy:

$$aAl_xGa_{(1-x)}As = axAlAs + a(1-x)GaAs \qquad \textbf{(III-5)}$$

Table III-3: Calculation of lattice parameter a(A°) by change of composition X

	x	$\mathbf{a(A^0)}$
GaAs	0	5.6530
$\mathbf{Al_XGa_{1-X}As}$	0.1	5.65381
	0.2	5.65462
	0.3	5.65543
	0.4	5.65624
	0.5	5.65705
	0.6	5.65786
	0.7	5.65867
	0.8	5.65948
	0.9	5.66029
AlAs	1	5.6611

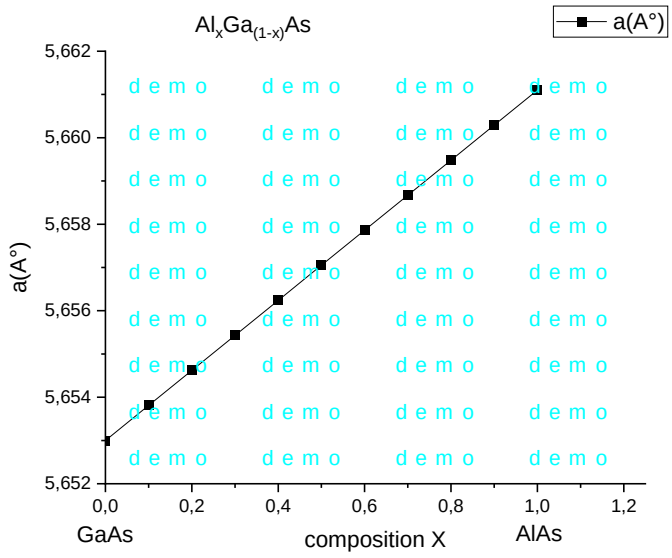

Figure III-5: the variation of lattice parameter a(A°) for $Al_XGa_{1-X}As$ alloy as a function of composition X

Figure III-5 shows us the changes of lattice parameter a(A°) in terms of the change in composition x, and these changes are linear and monotonous.

III.2.4 Electronic band structure

Study the electronic band structure of the $Al_XGa_{1-X}As$ alloy calculated at high symmetry points in the Brillouin region.

In order to be able to interpret the corresponding figures (III-6, III-7) illustrating the band structures of binary alloys, it should be noted that the zero energy reference is the maximum of the valence band.

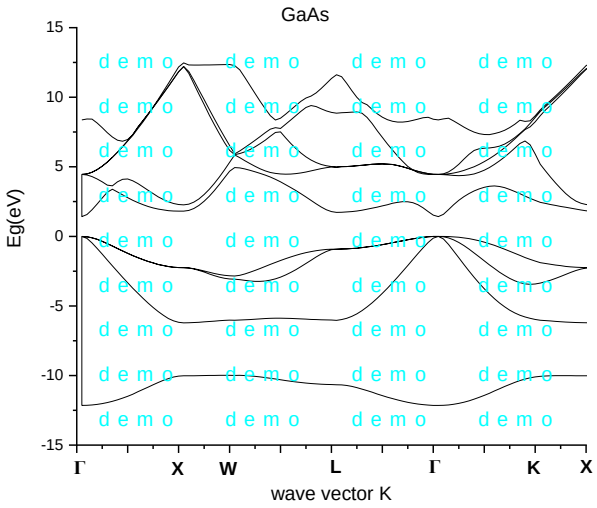

Figure III-6: Electronic band structure of the binary compound GaAs

In the figure (III-6), we notice that the maximum of the valence band is at the point Γ and that the minimum of the conduction band is also at the point Γ, from where the binary compound GaAs is a semi -conductor with direct bandgap, the difference noted between the minimum and the maximum is 1.42118 eV, and this coincides with the value reported in reference **[2]**.

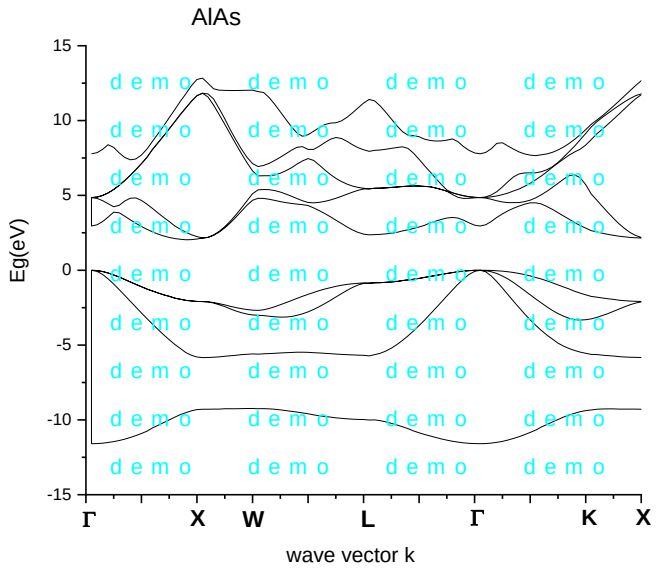

Figure III-7: Electronic band structure of the binary compound AlAs

In the figure (III-7) we see that the maximum of the valence band is at point Γ and that the minimum of the conduction band is also at point X, hence the binary compound AlAs is a semiconductor with indirect bandgap, the difference noted between the minimum and the maximum 2.14773 eV, and this coincides with the value reported in reference **[2]**.

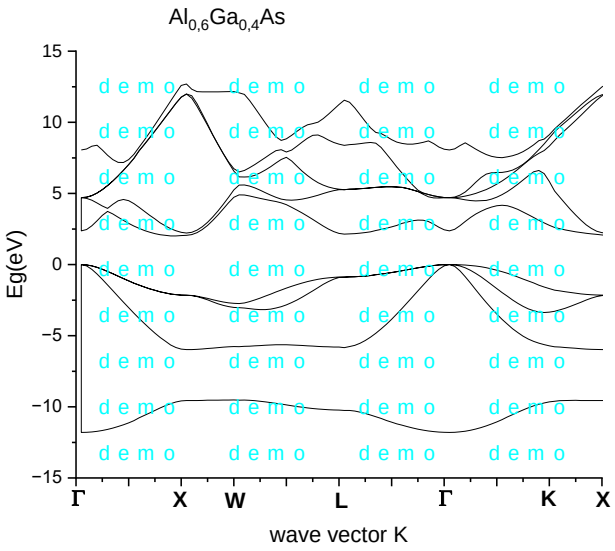

Figure III-8: Electronic band structure of the ternary compound $Al_XGa_{1-X}As$

The energy band structure of the ternary alloy $Al_{0.6}Ga_{0.4}As$, is schematized in figure (III-8) where the energy gap is indirect, and it is associated with the valley X, whose minimum is located at 2.05612 eV from the maximum of the valence band.

III.3 Study of optical properties

III.3.1 Refractive index

Using these five models, we calculated the refractive index of the $Al_XGa_{1-X}As$ semiconductor alloy from the values of their energy gap.

The results of our refractive index calculation for each model are presented in Table (III-4).

Table III-4 Calculation of the refractive indices of the $Al_XGa_{1-X}As$ alloy according to the composition x

	Model 01	**Model 02**	**Model 03**	**Model 04**	**Model 05**	**n epx**
GaAs	2.952556	3.2028684	2.9928913	3.2485607	2.951997	3.3 [a)]
$Al_XGa_{1-X}As$	2.692116	2.8092056	2.6857258	2.8356367	2.412298	
AlAs	2.662937	2.7524074	2.6475691	2.8792275	2.3344295	2.86 [a)]

where:

[a)] Theoretical value indicated in Ref :**[26]**

The variation of the refractive index of $Al_XGa_{1-X}As$ as a function of the composition **x** from different models is displayed in Figure III-9**.**

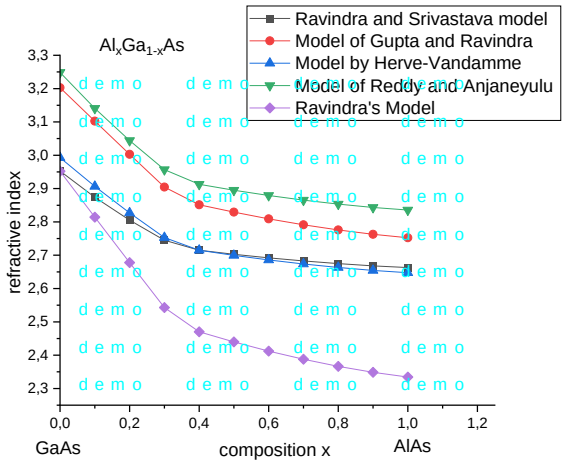

Figure III-9: the variation of the refractive index of $Al_XGa_{1-X}As$ as a function of the composition **x** of the Aluminum of the five models.

Figure (III-9) shows the change of refractive index of $Al_XGa_{1-X}As$ as a function of the x component of Aluminum in the five models.

We note that all models present the same behavior, refractive index decreasing with increasing composition **x** of Aluminum.

The decrease in refractive index is directly related to the value of the gap as a function of composition **x**. It decreases when the gap value increases.

For comparison, we have also presented the theoretical value cited in Ref [26].

The results from these comparisons are the best agreement between our results and the theoretical value according to the following relationship:

$$\Delta n/n = \frac{n_{exp} - n_{Calc}}{n_{exp}} \qquad \textbf{(III-6)}$$

Table III-5 Calculation of the variation for each refractive index of the $Al_XGa_{1-X}As$ alloy

	Δn1/n1	**Δn2/n2**	**Δn3/n3**	**Δn4/n4**	**Δn5/n5**
GaAs	0.10528606	0.029433818	0.093085060	0.01558766	0.10545545
AlAs	0.06890314	0.03761979	0.07427653	0.0067229	0.18376590

The best agreement between our results and the theoretical value of compound AlAs is given by the relations of the model of Gupta and Ravindra and that of Reddy and Anjaneyulu.

But it must be said that the model that gives the closest value to the theoretical value is the Reddy and Anjaneyulu model.

The best agreement between our results and the theoretical value of compound GaAs is given by the relations of the model of Gupta and Ravindra and the model of Reddy and Anjaneyulu.

But it must be said that the model that gives the closest value to the theoretical value is the Reddy and Anjaneyulu model.

Then we can conclude that the Reddy and Anjaneyulu is the most appropriate model for our ternary alloy $Al_XGa_{1-X}As$.

III.4 Study of dielectric properties

III.4.1 High frequency dielectric constant

Based on the calculated values of index **n** obtained from the Reddy and Anjaneyulu Model, the high frequency dielectric constant $\boldsymbol{\varepsilon_\infty}$, was estimated for different compositions x using the following expression:

$$\boldsymbol{\varepsilon_\infty = n^2} \qquad \textbf{(III-7)}$$

Table III-6 High frequency dielectric constant as a function of the composition x

	Model 04	$\boldsymbol{\varepsilon_\infty}$	**n exp**
GaAs	2.952556	10.553146	3.3 [a)]
$\mathbf{Al_{0.6}Ga_{0.4}As}$	2.692116		
AlAs	2.662937	8.289951	2.86 [a)]

where:

a) Theoretical value indicated in Ref :**[26]**

Calculating the refractive index (n) for the model chosen is Reddy and Anjaneyulu, the values of the high-frequency dielectric constant $\boldsymbol{\varepsilon_\infty}$ for GaAs and AlAs are 10.553146 and 8.289951.

We find that with increasing aluminum concentration, the value of $\boldsymbol{\varepsilon_\infty}$ decreases with increasing value of component x.

This is an expected result because ε∞ is obtained from equation III-7. The behavior of $\boldsymbol{\varepsilon_\infty}$with respect to x indicates that as soon as one proceeds from GaAs(x = 0) to AlAs (x = 1), the ternary alloy of interest (0 <x <1) gradually becomes a good conductor electric.

The variation of the constant ε∞ for the $Al_XGa_{1-X}As$ alloy from the different models, for different composition x of aluminum in the interval (0≤ x≤1) is presented in the following figure **III-10** :

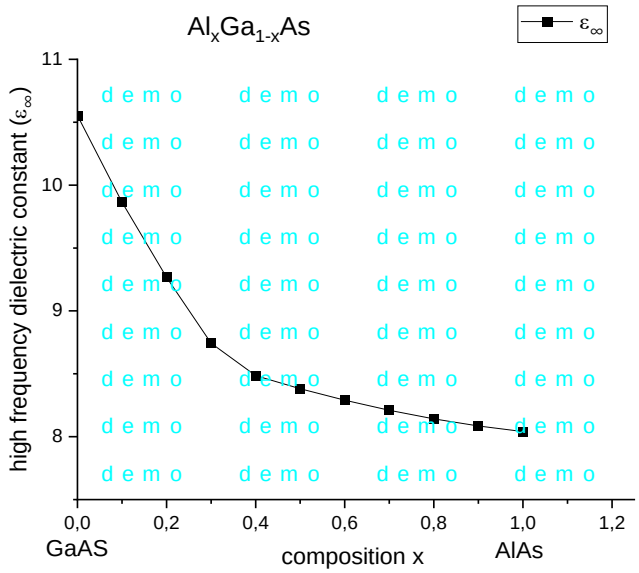

Figure III-10: The variation of the high frequency dielectric constant of the alloy $Al_XGa_{1-X}As$

Conclusion:

In this chapter, we have studied the electronic, optical and dielectric properties such as band gap, band structure, refractive index and high frequency dielectric constant of the ternary semiconductor alloy $Al_XGa_{1-X}As$. To do this, we used the experimental pseudopotential method combined with virtual crystal approximation. All properties have been checked against the x component of aluminum.

Whereas, the binary compound GaAs is a compound with a direct band gap and the compound AlAs is a compound with an indirect band gap.

The ternary compound $Al_XGa_{1-X}As$ is a compound with a direct bandgap of 0 to 0.3, and an indirect bandgap of 0.4 to 1 of the structure .

The refractive index is calculated according to the five existing models, it varies monotonically and linearly with the x component, The behavior is the same for the variation of the high-frequency dielectric constant with the x component.

General Conclusion

General conclusion

Through this work, we have studied the electrical, optical and structural properties of the $Al_xGa_{1-x}As$ ternary compound, and these properties have been studied and examined as a function of the change in the composition X of aluminum. The calculations are mainly performed using the empirical pseudopotential method EPM, together with the virtual crystal approximation VCA.

Our results show that for $Al_xGa_{1-x}As$, with lattice parameter ranging from 5.653 Å (GaAs) to 5.6611 Å (AlAs).

The direct (E_Γ^Γ) and indirect (E_X^Γ) (E_L^Γ) gaps exhibit the same behavior, as we have noticed that there is a transition between them. Since in the direct gap (E_Γ^Γ) its value ranges from 1.42118 to 1.9025 each time the transition varies from 0 to 0.3 of composition X, and in the indirect gap its value ranges from 1.98794 to 2.14773 each time the transition varies from 0.4 to 1 of composition X. The value of the direct (E_X^Γ) and indirect (E_X^Γ), (E_L^Γ) gap increases with the increase in composition X, and this increase is monotonous and linear.

The refractive index was calculated according to five experimental models. The change in refractive index as a function of the x composition of the tertiary semiconductor alloy $Al_XGa_{1-X}As$ showed a decrease in the refractive index as the aluminum component x increased for all models used. With the AlAs composite, the best agreement between our results and the theoretical value is that given by the Reddy and Anjaneyulu model, and for the GaAs composite, the Reddy and Anjaneyulu model gives the value closest to the theoretical value.

The high-frequency dielectric constant ε_∞ is calculated for the best model, and their behavior is calculated as a function of aluminum composition x, and it gradually decreases with increasing composition x.

Controlling these parameters by varying the x composition of the ternary alloy $Al_XGa_{1-X}As$ is of particular importance for the design of new optoelectronic devices and is of great importance for the future of semiconductor industry, especially in the field of renewable energy due to its optical properties.

Bibliographic references:

[1] Y.Y.Peter and M.Cardona, Fundamentalsof Semiconductors (Physics and Materials Properties), 4th ed., 2010.

[2] J. R. Meyer, L. R. Ram-Mohan and other, "Band parameters for III–V compound semiconductors and their alloys," *JOURNAL OF APPLIED PHYSICS*, 2001.

[3] M.Labidi, "Etude des propriétés structurales, électroniquesdes quaternaires.," 2011.

[4] D.A.Neamen, Semiconductor Physics and Devices, 4 ed., Raghu Srinivasan.

[5] J.M.Fiore, Semiconductor Devices:Theory and Application, 2021.

[6] B.Mohamed, "Technologie et integration ensemi-conducteurs iii-v," 2016

[7] A.AMINA, "Etude de quelques propriétés physiques de L'alliage BxIn1-xSb en utilisant les méthodes de premiers principes," 2019.

[8] D.K.BHOI, "study of zinc blende and wurtzite zns," *International Journal of Research in all Subjects in Multi Languages.*

[9] B.Nawel, "Etude des proprietes optoelectroniques des semiconducteursiii-v abase de galium.," 2010.

[10] S.Adachi, « Properties of Group IV, III-V and II-VI Semi-conducteur »

[11] N.M. Ravindra, V.K. Srivastava, Infrared Phy. 19 (1979) 603

[12].V.P. Gupta, N.M. Ravindra, Phys. Stat. Sol. (b) 100 (1980) 715

[13] P. Hervé, L.K.J. Vandamme, Infrared Phys. Technol. 35 (1994) 609

[14] R.R. Reddy, S.Anjaneyulu, Phys. Stat. Sol. (b) 174 (1992) K 91.

[15] M. Ravindra, P. Ganapathy, J.Choi, Infrared Phys. Technol. 50 (2007) 21.

[16] B.Yakout, "Etude théorique des propriétés structurales et électroniques des alliages BexMg1-xTe.," 2021.

[17] B.Samia, "Calcul de premier principe de quelques propriétés physiques de quelques alliages semi-conducteurs," 2016.

[18] B.Mohamed, "Propriétés structurale, élastiques et électronique d'alliages de nitrure desmétaux de transitions," 2014

[19] M.H.A.Hamza, "Exploration des alliages iii-v-nitrures (algan,bgan et baln) par algorithme évolutionnairecouplé à la théorie de la fonctionnelle de la densité," 2020.

[20] M.Amel, "Etude des propriétés structurales et électroniques del'alliage InxGa1-x Sb par la méthode ab-initioFP-LMTO," 2016.

[21] S.Riyadh, "Effet de la pression sur la structure et les propriétés diélectrique du composé semi-conducteur binaire CdTe," 2021.
[22] S.K.Tripathy and A.Pattanaiky, "Optical and electronic properties ofsome binary semiconductors fromenergy gaps," *Indira Gandhi Institute of Technology*,
[23] F. Mezrag, Thèse de doctorat, Univ Mohamed Khider Biskra (2012)
[24] H. A. N. Bouarissa, Infrared Physics & Technology, 1995.
[25] S.T.Murphy, C.Alexander, R.W.Grimes, C.Jiang and other, "Deviations from Vegard's law in ternary III-V alloys," *Physical Review B*, 2010.
[26] M. Levinshtein, S. Rumyantsev, M. Shur Eds.), Handbook Series on Semiconductor Parameters, vol. 2, World Scientific, Singapore, (1999)

Abstract

The aim of this work is to study the electronic, optical and dielectric properties of semiconductor alloys $Al_xGa_{1-x}As$ As in the structure of zinc blende, because these alloys have great importance in the future manufacturing of photovoltaic devices. For our calculations, we mainly relied on the empirical pseudo-potential approach combined with the virtual crystal approximation (VCA).

Our results showed that the alloy $Al_xGa_{1-x}As$ presents two energy gaps: a direct energy gap of 0 to 0.3 of the composition x, and an indirect energy gap of 0.4 to 1 depending on the change in aluminum concentration of composition x. Where this characteristic can offer the possibility of obtaining refractive index and dielectric constants.

Our results are in good agreement with other experimental and theoretical findings.

Key words: III-V semiconductors, $Al_xGa_{1-x}As$ alloy, empirical pseudo-potential (EPM), virtual crystal approximation (VCA).

résumé

Le but de ce travail est d'étudier les propriétés électroniques, optiques et diélectriques des alliages semi-conducteurs $Al_xGa_{1-x}As$ dans la structure du zinc blende, car ces alliages ont une grande importance dans l'avenir de la fabrication de dispositifs photovoltaïques. Pour nos calculs, nous nous sommes principalement appuyés sur l'approche empirique du pseudo-potentiel combinée à l'approximation du cristal virtuel (VCA).

Nos résultats ont montré que l'alliage $Al_xGa_{1-x}As$ présente deux gaps d'énergies : un gap énergétique direct de 0 à 0,3 de la composition x, et un gap énergétique indirect de 0,4 à 1 en fonction du changement de la concentration en aluminium de la composition x. Là où cette caractéristique peut offrir la possibilité d'obtenir des indices de réfraction et des constantes diélectriques.

Nos résultats concordent bien avec d'autres résultats expérimentaux et théoriques.

Mots clés : semi-conducteurs III-V, alliage AlxGa1-xAs, pseudo-potentiel empirique (EPM), approximation du cristal virtuel (VCA).

ملخص

الغرض من هذا العمل هو دراسة الخواص الإلكترونية والضوئية والعازلة لسبائك أشباه الموصلات $Al_xGa_{1-x}As$ كما هو الحال في بنية مزيج الزنك ، لأن هذه السبائك لها أهمية كبيرة في المستقبل. تصنيع الأجهزة الكهروضوئية . بالنسبة لحساباتنا ، اعتمدنا بشكل أساسي على نهج الإمكانات الزائفة التجريبية جنبًا إلى جنب مع التقريب البلوري الافتراضي (VCA).

أظهرت نتائجنا أن السبيكة $Al_xGa_{1-x}As$ كما تقدم فجوتين للطاقة: فجوة طاقة مباشرة من 0 إلى 0.3 من التركيبة x ، وفجوة طاقة غير مباشرة من 0.4 إلى 1 اعتمادًا على التغير في الألومنيوم تركيز التركيب x. حيث يمكن أن توفر هذه الخاصية إمكانية الحصول على مؤشرات انكسار وثوابت عازلة.

تتفق نتائجنا بشكل جيد مع النتائج التجريبية والنظرية الأخرى.

الكلمات الأساسية: أشباه الموصلات III-V ، سبيكة $Al_xGa_{1-x}As$ ، الإمكانات الزائفة التجريبية (EPM) ، التقريب البلوري الافتراضي (VCA).